SIMULATION OF SUPERCRITICAL WATER FLOW IN THE VENELLE 2 WELL

ALEXANDRE MORIN, BJØRN TORE LØVFALL, ERNST MEESE

ABSTRACT. We model a deep geothermal well in the commercial multiphase pipe flow simulator LedaFlow. The well is going to be drilled down to approximately 3000 m in a supercritical water reservoir. LedaFlow is developed for the oil and gas industry and is used amongst other to simulate oil and gas production wells. This makes it very well suited to simulate water/steam production wells. The model includes the surrounding rock layers, in which the heat transfer equation is solved dynamically.

We run both steady-state and transient cases. The steady-state cases show the potential for production of a well given the well geometry and the reservoir pressure, for different conditions at wellhead. In addition, we can retrieve the temperature profile in the casings, cement and rock at different distances from the well.

The transient cases are illustrations of phenomena that can take place in such a well. LedaFlow allows using a production index model for reservoir-to-well inflow, but here we keep the model simple: at bottomhole and wellhead, the boundary conditions are fixed pressure nodes. In addition, a valve can close the well at wellhead. We simulate start-up from a well in cold state (in equilibrium with the geothermal temperature profile) and in warm state (a well which has been producing shortly before), and show that the behaviour is very dependent on the thermal state of the well, due to the temperature dependence of the water/steam density. Also, we find that it may not be possible to avoid transitory phases of condensation in the well, and thus multiphase flow. Finally, we simulate shut-in, where the wellhead valve is closed to stop production. In this case, a temperature spike is seen, caused by compression of the steam.

1. INTRODUCTION

Geothermal energy has the potential to offer a competitive and significant clean contribution to the energy mix (cf. for example, for Europe, the report of the GEOELEC project [1]). There is a broad range of applications, shallow or deep, with a heat pump or not, water injection-production or production of geological water, direct use of heat or electricity production. In particular, high-temperature geothermy is well suited for electricity production, especially for base-load. The production of geothermal electricity in the EU in 2013 is 6 TWh, while the potential in 2030 is 174 TWh, according to the GEOELEC report [1], and in 2050, more than 4000 TWh.

One of the obstacle to the development of geothermal electricity production is the cost of drilling the well. Thus, most of the ongoing research activities focus on that part. The European project Descramble [2] aims for example at drilling a well into a reservoir of supercritical water in Italy (critical point of water: 374 °C, 220.64 bar). Producing supercritical water would allow increasing the power capacity per well by an order of magnitude [3, p. 26], thus diluting accordingly the drilling costs. However, when the issue of drilling is overcome, challenges related to operation need to be addressed. In the Oil and Gas industry, this is known as Flow Assurance.

Liquid in gas flows (as a film or as droplets) implies some technological challenges, especially in vertical pipes, as the liquid has to be carried upwards by the gas phase. In addition, the equipment, for example valves, has to be specially designed for operation in multiphase flow. Thus, for technological simplicity, one would rather produce in single phase in steady state. However, during transient events, like start-up or shut-in, it may not be possible to avoid multiphase flow. For these cases, a multiphase pipe flow simulator will help designing and controlling the well in order to ensure efficiency and safety.

In the present article, we aim at demonstrating the ability of the commercial pipeline multiphase flow simulator LedaFlow [4, 5] to model the flows relevant for deep geothermal wells, that is, flows of water with phase change, included in supercritical state. In further work, it will be of interest to include impurities in the water, mostly CO_2, but this is not in the scope of the present article. Dynamic heat transfer in the surrounding rock is taken into account. LedaFlow was initially developed for the oil and gas industry, one of its core applications being the simulation of oil and gas production wells. This makes it very well suited to simulate geothermal wells. In the present work, we use as an example the Venelle 2 well from the Descramble project. The well will be drilled further down to a depth of about 3000 m, in order to reach a high pressure supercritical water reservoir. The water flow in the well under production is simulated with LedaFlow, where a thermodynamic property table for single-component water, covering pressures and temperatures high in the supercritical region, has been integrated for this purpose. Three types of cases are simulated

- Steady-state cases predict the water conditions at wellhead given a reservoir pressure and temperature, particularly the mass flow rate resulting from regulating the wellhead pressure at a given target value, and its temperature. This is what is needed to evaluate the power that can be generated from the well. In addition, the simulations give the temperature profile in the well and in the surrounding rock at a given distance from the well.
- In start-up cases, the well is initialised as if there had been stagnant water in the well for a long time. This means that the water temperature follows the geothermal gradient, and that the wellhead pressure is the bottom hole pressure, subtracted with the hydrostatic pressure difference in the well. Then, the top valve is opened and the well can start producing. The evolution of pressure and temperature, both in the fluid and the surrounding rock, is predicted.
- Shut-in cases simulate the temperature spike observed when the wellhead valve is closed during steady state production.

These cases are run assuming bottom hole pressures in [150, 250, 350, 450] bar. The water temperature at the bottom hole is always 450°C. The transient cases are defined to illustrate some phenomena that are useful to be aware of, and show the possibilities of a multiphase well flow simulator for flow assurance, process control and safety analysis. For actual applications, the well model will have to be completed to reflect the equipment design and technological choices.

In Section 2, LedaFlow is presented as well as the models that it solves. The physical models relevant to multiphase flow are also explained. In Section 3, the model of the Venelle 2 well is detailed. Then, in Section 4, numerical results are presented for the steady-state and transient cases.

2. LedaFlow

LedaFlow is a commercial multiphase pipe flow simulator primarily developed for oil and gas applications (see for example [4, 5]). It can handle three-phase flows

of gas, oil and water, but can also be run in two-phase mode, the latter being the most relevant for geothermal applications. The model also accounts for dispersed phases. For vertical two-phase, steam-water flows, this means that the following situations, amongst other, can be simulated:

- A liquid film on the walls with steam flowing in the middle, with droplets entrained in the steam and possibly steam bubbles in the liquid,
- A bubbly flow,
- An intermittent flow of liquid with large bubbles periodically rising in the liquid.

One mass equation is solved for each of the phases (including the dispersed phases), with transfer terms for mechanical mass exchange and phase change. For the momentum and energy equations, the dispersed phases are solved together with the phase they are dispersed in. Thus, in the first steam-water flow example above, one momentum equation is solved for the steam including droplets, and one for the liquid film including bubbles. For dispersed phases having a different velocity than the phase they travel in, for example bubbles rising in water, an algebraic relation is applied for the relative velocity. Concerning the energy equations, this implies that the dispersed phases are in thermal equilibrium at all times with their bearing phase. This is a reasonable assumption as the time scales of the flow are larger than the time scales for heat exchange between the dispersed phases and their bearing phase.

The fluid-dynamical model which is solved is the multifluid model. For example, for the a two-phase case, the equations are as follows. The mass conservation equations are

$$(2.1) \qquad \frac{\partial}{\partial t}\left(\alpha_k \rho_k\right) + \frac{\partial}{\partial x}\left(\alpha_k \rho_k u_k\right) = \sum_{m \neq k} \Gamma_{m \to k} + \Gamma_{k,\text{ext}},$$

where α_k is the phase volume fraction, ρ_k is the phase density, u_k is the phase velocity, Γ_{km} and $\Gamma_{k,\text{ext}}$ are the mass exchange source terms, respectively between phases and with the outside (for example, well inflow). k refers to the phase, thus for water, steam, droplets and bubbles, $k \in [1,4]$. Then, the momentum equations are

$$(2.2) \quad \frac{\partial}{\partial t}\left(\alpha_k \rho_k u_k\right) + \frac{\partial}{\partial x}\left(\alpha_k \rho_k u_k u_k\right) = -\alpha_k \frac{\partial p}{\partial x} - \Phi_k \frac{\partial h_l}{\partial x} - \alpha_k \rho_k g \sin \theta$$
$$+ \sum_{m \neq k} F_{km}^i + F_k^w + \sum_{m \neq k} \left(\Gamma_{m \to k} u_m - \Gamma_{k \to m} u_k\right) + \Gamma_{\text{ext} \to k} u_{k,\text{ext}} - \Gamma_{k \to \text{ext}} u_k,$$

where p is the pressure, h_l is the liquid level, which together with the coefficient Φ_k gives the hydraulic force making surface waves propagate, g is the gravity constant, θ is the angle that the pipe makes with the horizontal, and F^i and F^w are the interfacial and wall friction forces, respectively. The hydraulic force coefficient is defined as

$$(2.3) \qquad \Phi_k = \begin{cases} \alpha_l \left(\rho_l - \rho_g\right) g \cos \theta & \text{if } k = l, \\ 0 & \text{if } k = g. \end{cases}$$

Note that it is close to zero for nearly vertical flows, thus is it not very relevant for well flows. The mass exchange source terms Γ_{km} have been split based on direction: to phase k, $\Gamma_{m \to k}$, or from phase k, $\Gamma_{k \to m}$. The same is done the the exchange with the outside. Finally, the energy equations are expressed in terms of total enthalpy

$$(2.4) \qquad H_k = h_k + \frac{1}{2} u_k^2 + gz,$$

as

$$(2.5) \quad \frac{\partial}{\partial t}\left(\alpha_k \rho_k H_k\right) + \frac{\partial}{\partial x}\left(\alpha_k \rho_k H_k u_k\right) = \alpha_k \frac{\partial p}{\partial t} + \sum_{k \neq m} Q^i_{km} + Q^w_{kw}$$

$$+ \sum_{m \neq k}\left(\Gamma_{m \to k} H_m - \Gamma_{k \to m} H_k\right) + \Gamma_{\text{ext} \to k} H_{k,\text{ext}}, + \Gamma_{k \to \text{ext}} H_k,$$

where h_k is the specific enthalpy, z the height, and Q^i and Q^w are the interfacial and wall heat transfer rates, respectively.

2.1. **Physical models.** The physical models in LedaFlow are based on extensive experimental data and cover the flow rates and flow conditions relevant for pipe and well flows. In LedaFlow, they are based on a flow regime map. First, a flow regime is determined based on the local flow conditions, then the characteristics of the flow like volume fraction of steam, friction, heat transfer, *etc.* are evaluated and used to close the equation system of the previous section. The possible flow regimes in nearly-vertical pipes are

- Annular flow,
- Slug flow,
- Bubbly flow.

2.2. **Heat transfer to surroundings.** In addition to the physical models for heat transfer between the phases and to the walls, the heat balance in the model is simulated with a transient heat transfer model in the material layers around the well (casings, cement and rock). Note that axial heat transfer is for the time being neglected.

2.3. **Thermodynamic model.** The fluid-dynamical model uses a tabulated steam-water equation of state, and can handle subcritical as well as supercritical phases. As explained above, an energy equation is solved for each bearing phase with its dispersed phases. Thus, the liquid film and the gas core may be in thermal inequilibrium, while exchanging heat and mass .

2.4. **Liquid transport.** With the heat transfer model it is possible to predict steam condensation in the well. When this happens, it is expected to condensate on the walls, as a liquid film. However, depending on the steam velocity, droplets may be entrained in the gas core. Empirical correlations govern the interfacial friction between the gas core and the liquid film, as well as the rate of entrainment and deposition of droplets. Thus, the model is able to predict the carrying of liquid upwards by the gas, or if it should happen, the accumulation of liquid in the well. The latter may lead to killing the well, in the case where the hydrostatic weight of the fluid column in the well counteracts the reservoir pressure.

In addition, the ability of the gas to transport the liquid upwards will determine the volume fraction of liquid, thus playing a significant part in the overall pressure drop in the well. In this respect, the last model developments in LedaFlow [6] focussing on vertical flows with very low levels of liquid are especially relevant for geothermal conditions.

3. The model

The present article uses as an example the Venelle 2 well to be further drilled in the Descramble project [2]. Figure 3.1 shows the profile of the well. It consists of five casings or liner separated by cement, reaching different depths. The lower part of the well is directly in contact with the rock. The inner liner has a diameter of 7 inches. In the present study, the total depth is taken to be 3000 m.
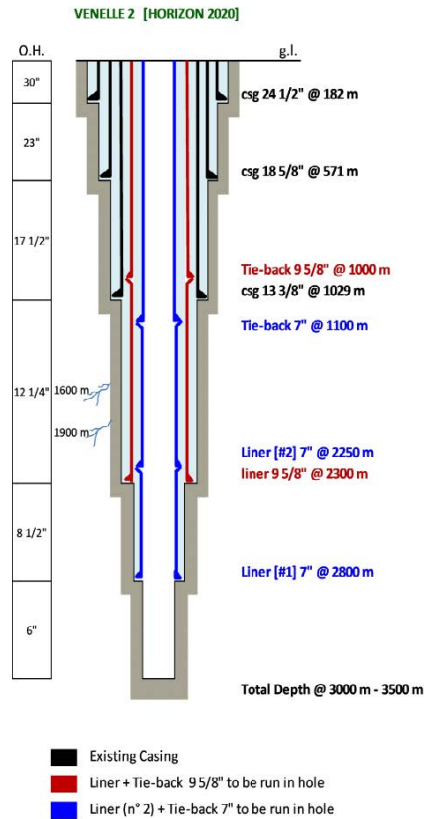
FIGURE 3.1. Profile of the Venelle 2 well after further drilling in
the Descramble European project [2]

The Venelle 2 well is modelled as shown in Figure 3.2. The pipe is directed
downwards (thus, the reported mass flow rates are negative if the flow is upward,
as expected). The pipe is meshed with 100 vertical cells. The well, and particularly
its boundary conditions, can be modelled in different ways, with different levels of
detail. For example, the reservoir acts, in a first approximation, like an imposed-
pressure boundary condition. However, the actual pressure at the well bottomhole
is dependent on the flow rate in the reservoir porous material in the near-well area.
Production index reservoir models are available in LedaFlow, but in this initial
study we are focussing on intrinsic well-phenomena and wish to keep the complexity
at a low level. Hence, a constant pressure inlet boundary condition has been used
at the bottomhole. Similarly, the wellhead equipment would typically regulate the
flow in the well according to some constraint. In the present study, we rather use
a pressure imposed boundary condition at the top and check the resulting flow in
the well. By varying the wellhead pressure level, we can cover different possible
flow rates. In addition, a valve is placed at wellhead, which is either fully-closed or
fully-opened, to study simple transient events like start-up and shut-in. Then, the
resulting mass flow rate is an output of the model.

The liners, casings, cement and rock layers are modelled as annular cells around
the pipe. The cells are divided vertically with the same mesh as the pipe, thus
there are 100 cells in this direction. Each liner, casing or cement layer is modelled
with one annular cell. The rock layers are modelled with 12 annular cells, up to
a distance of 100 m from the well. At the outside boundary of the rock layers,
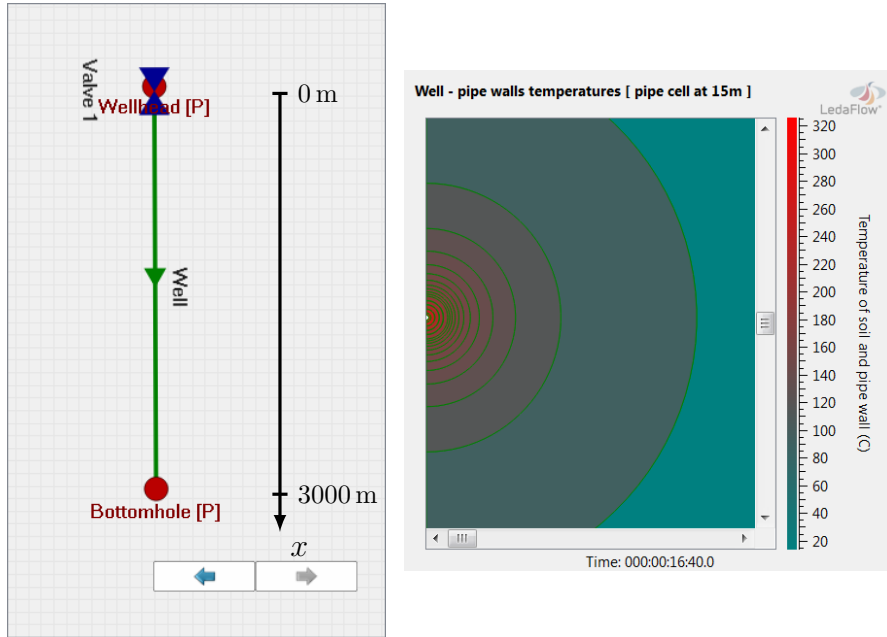
FIGURE 3.2. Model of the Venelle well and cross-section view (at 15 m depth) of the casings, cement layers and rock around

the geothermal profile shown in Figure 3.3 is applied. The heat equation is solved dynamically in the material mesh. This means that the temperature in the cylinder of 100 m of rock around the pipe will evolve in a transient way with the flow in the well.
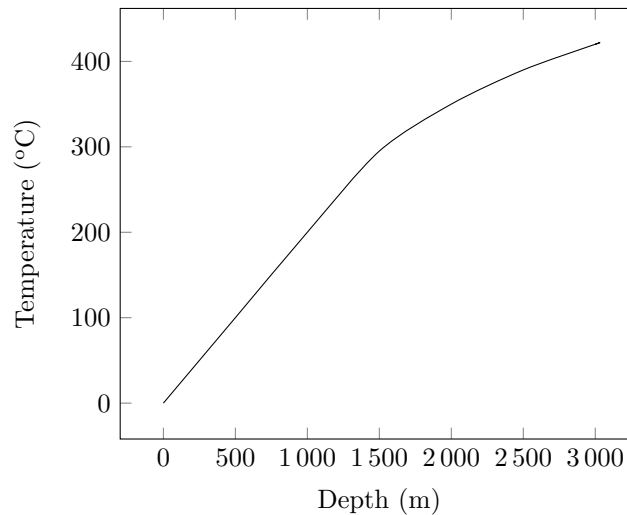

FIGURE 3.3. Geothermal profile at Venelle 2 site.

4. SIMULATION RESULTS

The Venelle 2 well has been simulated following different scenarios. First, steady-state cases have been run to assess the potential of production of the well and

the thermal conditions in the material and rock layers. Several levels of reservoir pressure have been tested, with a range of wellhead pressure levels. Second, some simplified transient cases have been run to test the reaction of the well.

4.1. **Steady-state cases.** In these cases, the simulation is initialised in steady state. Thus, this corresponds to the final temperatures, pressures and mass flow rates asymptotically reached in the well and rock around. The bottom hole pressure was set to the following values: [150,250,350,450] bar. For each of these bottom hole pressures, the wellhead pressure was varied by 40 bar steps. For each bottomhole pressure, the range of wellhead pressure levels was limited so that the well always flow upwards (a wellhead pressure too high would mean that we are pumping water down). Also, a too low wellhead pressure leads to technologically irrelevant fluid velocities. The ranges presented already extend beyond the sensible threshold.

In Figures 4.1, the well pressure-temperature profiles are plotted together with the saturation line. Remark that the two first cases, with low bottom hole pressures, do not meet the saturation line for any wellhead pressure, while the cases with higher bottom hole pressure do. Then, a mixture of steam with condensed liquid is produced by the well, and in the top section of the well, the pressure-temperature profile follows the equilibrium line.

Well pressure-temperature profile in steady state

(A) Bottom hole pressure 150 bar

(B) Bottom hole pressure 250 bar

(C) Bottom hole pressure 350 bar
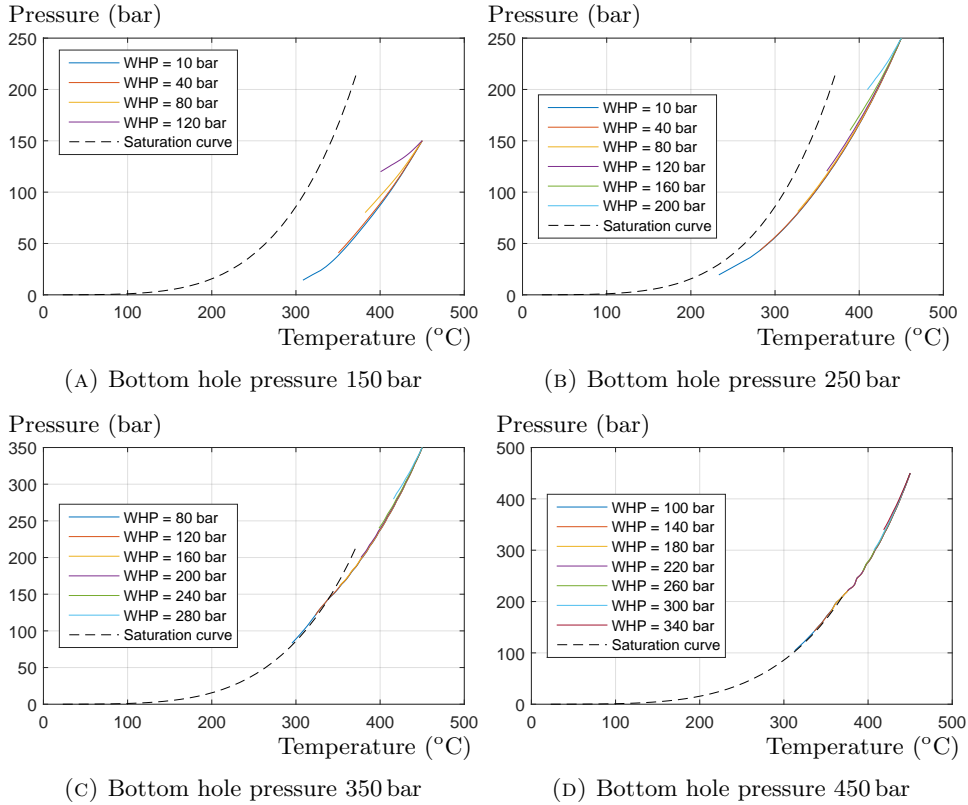
(D) Bottom hole pressure 450 bar

FIGURE 4.1. Well pressure-temperature profile in steady state for various wellhead pressures.

4.1.1. *Flow rate and temperature at wellhead.* The mass and volume flow rates for given bottom hole and wellhead pressures are plotted in Figures 4.2a–4.2b. The

total flow rates are plotted in solid lines, while the gas flow rates are plotted in dashed lines, when it is different from the total flow rate. The plots show that the total flow rate keeps on increasing as the wellhead pressure is decreased, but an increasing part is liquid. Due to the density difference between steam and water, the liquid mass flow rate is significant when condensation starts, but the volume of liquid water is still very small. Concerning the volume flow rate, it increases drastically for low wellhead pressures. This is due to the steam expansion at low pressure. The temperature at wellhead is plotted in Figure 4.2c.
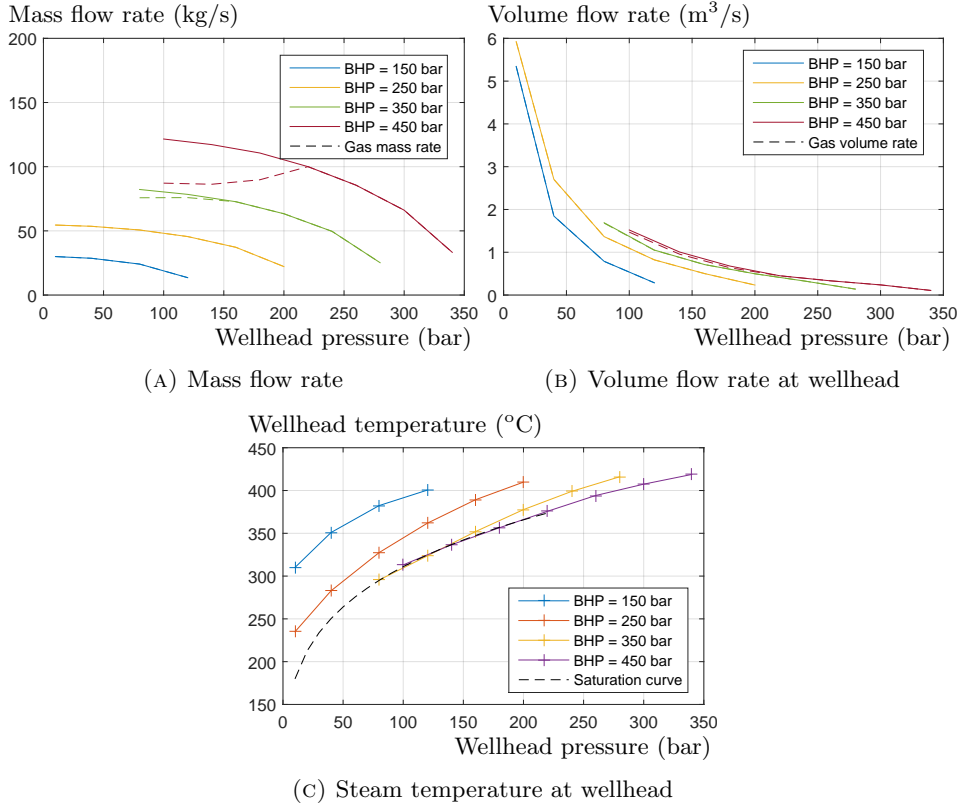

(A) Mass flow rate

(B) Volume flow rate at wellhead

(C) Steam temperature at wellhead

FIGURE 4.2. Well properties at constant bottomhole pressure.

4.1.2. *Enthalpy.* In terms of energy content, the well flow can be seen in a first approximation as an adiabatic expansion from the reservoir to the wellhead, but where the increase in potential energy from the reservoir depth to the surface is supplied by the fluid enthalpy. Kinetic energy is neglected. Thus, the specific enthalpy at the wellhead will be close to the specific enthalpy of the water in the reservoir, corrected for potential energy. However, friction and heat transfer to the surrounding rock cause some losses that decrease the specific enthalpy at wellhead. In Figure 4.3a, the specific enthalpy at the wellhead is plotted. The previous remark explains their shapes, more specifically

- At low flow rates (high wellhead pressures), the fluid residence time in the well is high, thus the heat loss to the terrain increases.
- At high flow rates (low wellhead pressures), the flow velocity is high, thus friction losses are high.

Note that the specific enthalpy decreases with higher pressure in the reservoir. At a given temperature, increased pressure means that the supercritical water is more and more liquid-like.

(A) Specific enthalpy at wellhead

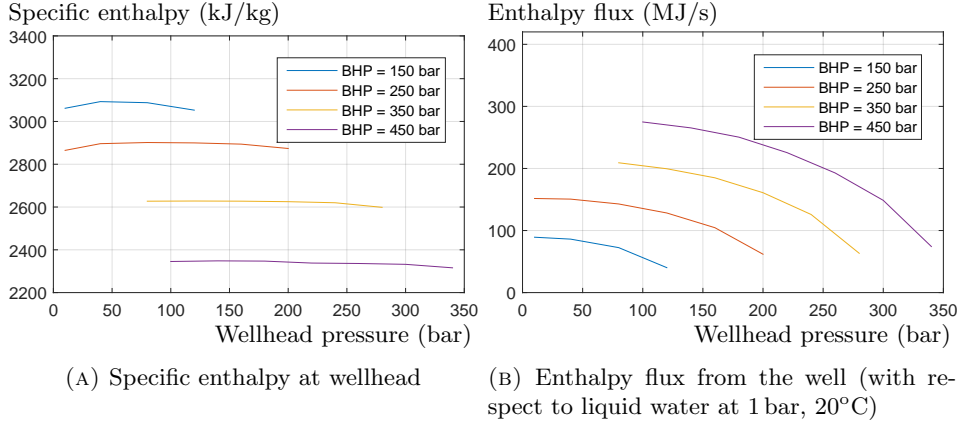(B) Enthalpy flux from the well (with respect to liquid water at 1 bar, 20°C)

FIGURE 4.3. Energy output of the well at constant bottomhole pressure.

It can be interesting then to look at the enthalpy flux, which together with the fluid temperature at wellhead, will determine the maximum theoretical electric power that can be generated from the well. This is dependent on the technology used for power conversion, but taking as a reference liquid water at 1 bar and 20°C, Figure 4.3b gives an idea of the thermal power out of the well. Here, the highest thermal flux out of the well is obtained for the highest reservoir pressure, which can be explained by a higher mass flow rate (due to a higher water density, cf. Figure 4.2a), even though the specific enthlapy of the produced water is lower than for lower reservoir pressures. Also, the enthalpy flux increases for decreasing wellhead pressure, even when condensation happens. This is also caused by a higher mass flow rate. However, this also implies a lower wellhead temperature (cf. Figure 4.2c), which decreases the theoretical maximum yield for electricity production.

4.1.3. *Temperature profile in the rock.* An example of temperature profile in the material layers at different distances from the well centerline is shown in Figure 4.4. The jumps in the temperature profiles are caused by changes in materials around the well (end of casing, change of rock type, *etc.*)

4.2. **Start-up from cold well.** In this simulation, the well is initialised with a closed wellhead valve, and the fluid, rock and pipe layers are initialised with the geothermal gradient. This corresponds to the situation where the well is filled with stagnant water, at thermal equilibrium with the surroundings. Then, the valve is fully opened (opening time 10 s) and the transient behaviour of the well is analyzed.

A simplified scenario has been defined: the wellhead pressure is set to a given value, and the wellhead valve is opened. This imposes a constraint on the wellhead pressure, as the well must start producing spontaneously. The imposed wellhead pressure must indeed be lower than the wellhead pressure occuring with closed valve (hydrostatic pressure gradient in cold well, plotted in Figure 4.5). Otherwise, there will be injection instead of production. Note that during production, the water in the well is warmer than in the closed cold well, so the hydrostatic pressure gradient is reduced. Hence, after the well has started producing, the wellhead pressure in steady-state production may be increased above the maximum pressure for start-up.
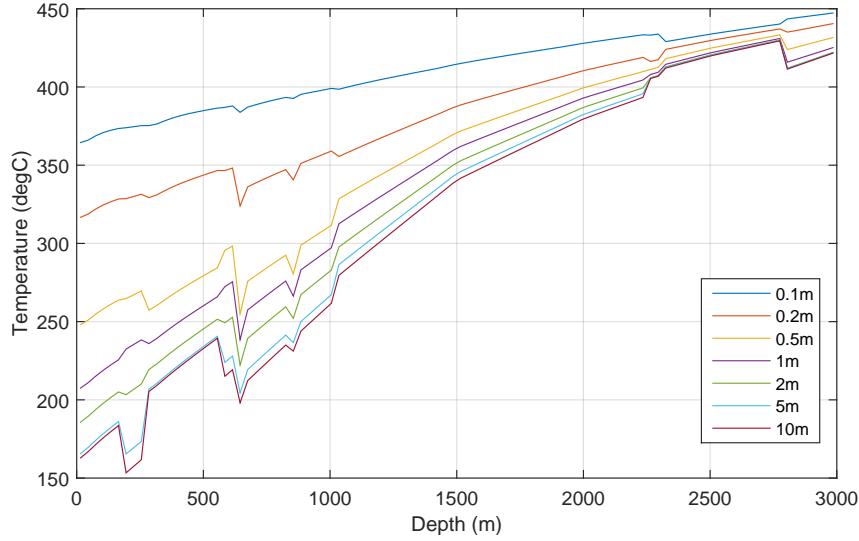
FIGURE 4.4. Temperature profile in the rock at different distances from the well centerline (BHP=450 bar, WHP=220 bar)

During start-up, the pressure-temperature profile will evolve from the stagnant profile in Figure 4.5 to the situation in Figures 4.1a–4.1d. Since the wellhead pressure in the stagnant well for a bottomhole pressure of 450 bar is higher than the critical point of water, it is possible with the chosen scenario to start this well and keep it entirely in single phase over the whole procedure. This is not possible with this simple scenario for lower levels of bottomhole pressure, as the wellhead pressure will cross the saturation line. In the present study, we will allow this and look at the reaction of the well in two-phase conditions.

It is, however, possible to define a scenario that would take the profile around the critical point, thus ensuring a single-phase flow at all times. First, the well is started with a wellhead pressure below the level observed in cold stagnating water. Then, as the liquid column warms up, the hydrostatic weight of the column decreases and the mass flow increases at constant wellhead pressure. Thus, the wellhead pressure can be progressively increased to a supercritical pressure. Then, when the well is warm enough, the wellhead pressure can be decreased again to increase production, and the profile will stretch into the steam region, without crossing the saturation line. Still, this may not be possible for the 250 bar bottomhole pressure case, as Figure 4.1b shows that the highest wellhead pressure in steady-state (200 bar) is below the critical pressure. It may not be possible to lead the wellhead above the critical point.

4.2.1. *Example of start-up (BHP=350 bar, WHP=120 bar).* The case presented here was run with a bottomhole pressure of 350 bar and a wellhead pressure of 120 bar. Figure 4.6 shows the results at the wellhead and at 500 m depth (or the closest numerical node). Figure 4.6a shows the mass and volume flow rates during the start-up from cold well. We can see a transient situation, before the flow rates stabilise after $t = 500$ s. Note that the liquid flow rate is not zero after the flow has stabilised, which means that there are some liquid droplets or a liquid film at wellhead. In the period before the flow rates have stabilised, we can see an increase in flow rate over 300 s before stabilising. However, whereas the mass flow peaks at more than four times its final value, the volume flow stabilises close to its peak value. This is because the mass flow rate peak is caused mainly by dense cold water
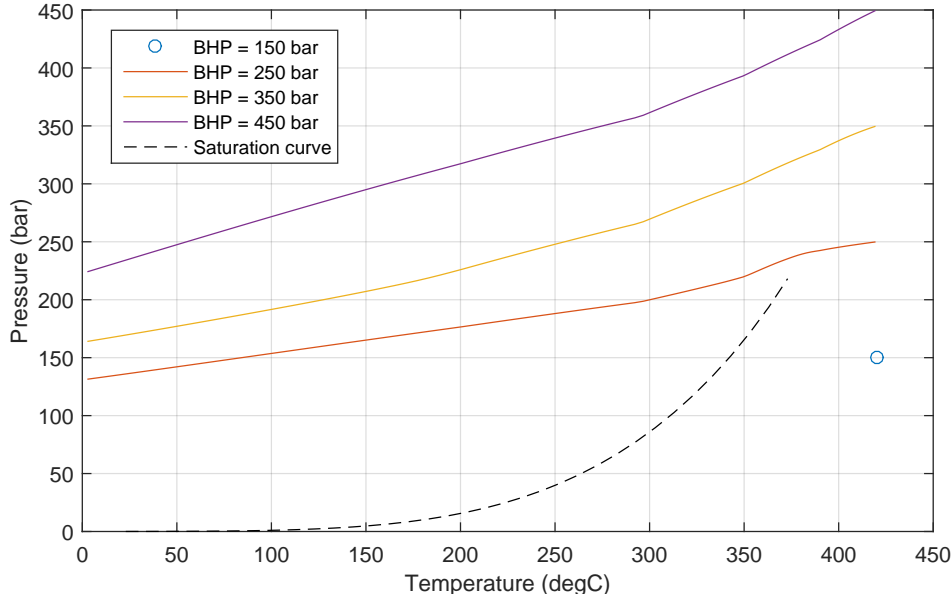
FIGURE 4.5. Hydrostatic pressure-temperature profiles of the cold well at different bottom hole pressures. The hydrostatic profile is undefined for BHP=150 bar, as it would imply that liquid water should rest on top of steam.

being flushed out and replaced by lighter steam. The volume flow rate is related to the flow velocity and does not peak in the same way. Note that during the flow rate acceleration, the flow is in single phase (liquid mass flow rate equal to total mass flow rate), while the flow is two-phase after the peak.

Figure 4.6c shows the pressures and temperatures for the cold start-up. We can see that the pressure drops from the initial wellhead pressure in hydrostatic equilibrium (≈ 133 bar) to the imposed wellhead pressure of 120 bar. Then, the temperature increases at wellhead, due to warmer water flowing upwards. Between 300 s and 600 s, the welhead pressure is unstable. This is caused by instabilities further down in the well, where the conditions are just above the critical point, a region where the density of the fluid is very sensitive to the pressure and the temperature. The density can vary from 300 kg/m^3 to 600 kg/m^3 over a few bars. This is challenging for the numerical scheme, as a cell may oscillate between two density levels, thus causing these pressure oscillations. Whether this behaviour would also be observed in reality is however unclear. Note that these pressure oscillations are coupled with the flow rate oscillations in Figure 4.6a.

4.3. **Restart of warm well.** This case is similar to the previous case, but it differs from start-up from the cold well in that the well has been operated long enough to have reached steady-state temperature in the rock layers. In practice, this is done in the simulation by initialising the well in steady-state production. Then, the flow is stopped by closing the valve and reopening it after 500 s (closing/opening time 10 s). The main consequence is that the temperature of the water or steam in the well right before start-up is very different. This has a strong effect on the density of the liquid column, thus affects the start-up dynamics.

4.3.1. *Example of restart of warm well (BHP=350 bar, WHP=120 bar).* When starting from warm well (Figure 4.7), we see that the flow rate increases much more

(A) Volume and mass flow rates at $\approx 0\,\mathrm{m}$

(B) Volume and mass flow rates at $\approx 500\,\mathrm{m}$

— Total volume flow rate   — Total mass flow rate

— Liquid volume flow rate   — Liquid mass flow rate

(C) Pressure and temperature of fluid, and wall temperatures at $\approx 0\,\mathrm{m}$

(D) Pressure and temperature of fluid, and wall temperatures at $\approx 500\,\mathrm{m}$

— Pressure   — Fluid temperature

— Temperature liner 7in   — Temperature liner 9in5/8
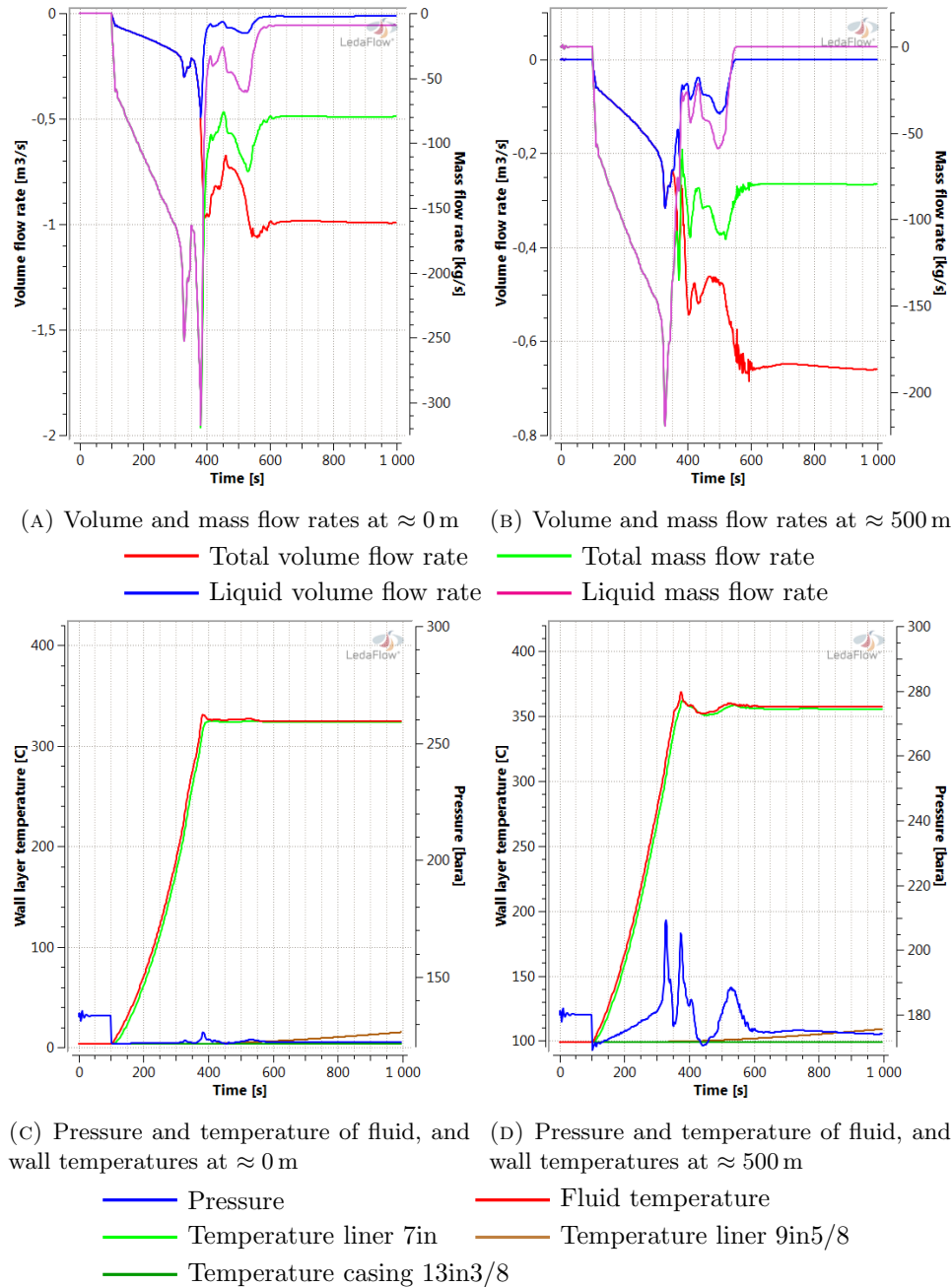
— Temperature casing 13in3/8

FIGURE 4.6. Well behaviour during start-up from cold well.

quickly (a few seconds instead of 300 s). There is also a peak in volume flow rate of twice the final flow rate (and thus a peak in velocity). Since the steam has not had the time to cool down, the steam density is much lower than in the cold start-up scenario, thus the hydrostatic pressure gradient is lower. This gives a larger pressure difference over the wellhead valve when it is opened. This also means that the production could be restarted at a higher wellhead pressure in the warm start-up scenario, since the hydrostatic pressure gradient to overcome is smaller. The exact

start-up scenario will however be dependent on the wellhead design. The LedaFlow model can be adapted accordingly to simulate a relevant scenario.

Figure 4.7c shows the pressures and temperatures for the warm start-up. The flow quickly reaches the equilibrium production values from before the shut-in. The shut-in in itself will be discussed in the following section. Concerning the minimum pressure necessary to start up the well, comparing Figures 4.6c and 4.7c shows that the state of the well has a significant influence. We can see that the pressure at wellhead before opening the valve is about 133 bar in the cold case, while it is about 280 bar in the warm case (it would gradually return to 133 bar as the well cools down). Thus, the warm well can be started with any wellhead pressure below 280 bar (thus limiting the amount of condensed water), while a wellhead pressure below 133 bar is necessary to start the cold well.

Note however, that the extreme compressibility of water just above the critical point ($300 \, \text{kg/m}^3$ to $600 \, \text{kg/m}^3$ over a few bar) is challenging to the numerical scheme. This causes the instabilities seen in Figure 4.7a, which start further down in the well, where the conditions are in the challenging region. Still, the real solution is within the instability range. Thus, the solution is still to be trusted.

4.4. **Shut-in from steady state.** In this simulation, we start from steady-state production, and close the valve at wellhead (closing time 100 s). Thus, the well pressure-temperature profile will travel from the steady-state production profiles (Figures 4.1a–4.1d) to the stagnating hydrostatic profiles (Figure 4.5). In general, it will cross the saturation line. It may be possible to control the wellhead pressure during the shut-in to go around the critical point to avoid two-phase flow, like proposed for the start-up. However, this means that one has to wait for the surroundings to cool down the water, which may take a long time. This has not been tried. In the present paper, we are keeping a simple scenario. The general behaviour is that a temporary increase in fluid temperature can be observed, caused by an increase in pressure, before cooling down to the surrounding temperature. The liner immediately in contact with the water follows almost the same trend. The second liner does almost not see any temperature increase.

4.4.1. *Example of shut-in (BHP=350 bar, WHP=200 bar or 80 bar).* Two cases are presented, both with 350 bar at bottomhole, one with 200 bar at wellhead and the other 80 bar. Trend curves are plotted for the water temperature and pressure during one day after the shut-in has taken place, as well as the temperature of the three first liners and casings, at three different depths in the well (Figures 4.8 and 4.9).

We can see that just after the shut-in, there is in both cases a peak in pressure and temperature, and the temperature of the liner directly in contact with the fluid follows closely the fluid temperature. In both cases, the pressure peaks at about 280–290 bar, before slowly decreasing as the fluid cools down and the hydrostatic pressure gradient of the liquid column increases. The peak temperature is also not very different between the two cases. The difference is that the jumps in themselves are more intense for the case with 80 bar at wellhead. There, the temperature jumps by 110°C, while the jump is only 30°C with 200 bar at wellhead.

Note also here that there are signs of instabilities in these cases too, in particular in Figure 4.8c at $t = 2$ hr and in Figure 4.8e at $t = 3$ hr.

5. Conclusion

Producing from supercritical water reservoirs for geothermal electricity production may allow increasing the energy through-put per well by an order of magnitude. The main technological challenge for the time being is the drilling. However, when

(A) Volume and mass flow rates at $\approx 0\,\mathrm{m}$

(B) Volume and mass flow rates at $\approx 500\,\mathrm{m}$

- Total volume flow rate
- Total mass flow rate
- Liquid volume flow rate
- Liquid mass flow rate

(C) Pressure and temperature of fluid, and wall temperatures at $\approx 0\,\mathrm{m}$

(D) Pressure and temperature of fluid, and wall temperatures at $\approx 500\,\mathrm{m}$

- Pressure
- Fluid temperature
- Temperature liner 7in
- Temperature liner 9in5/8
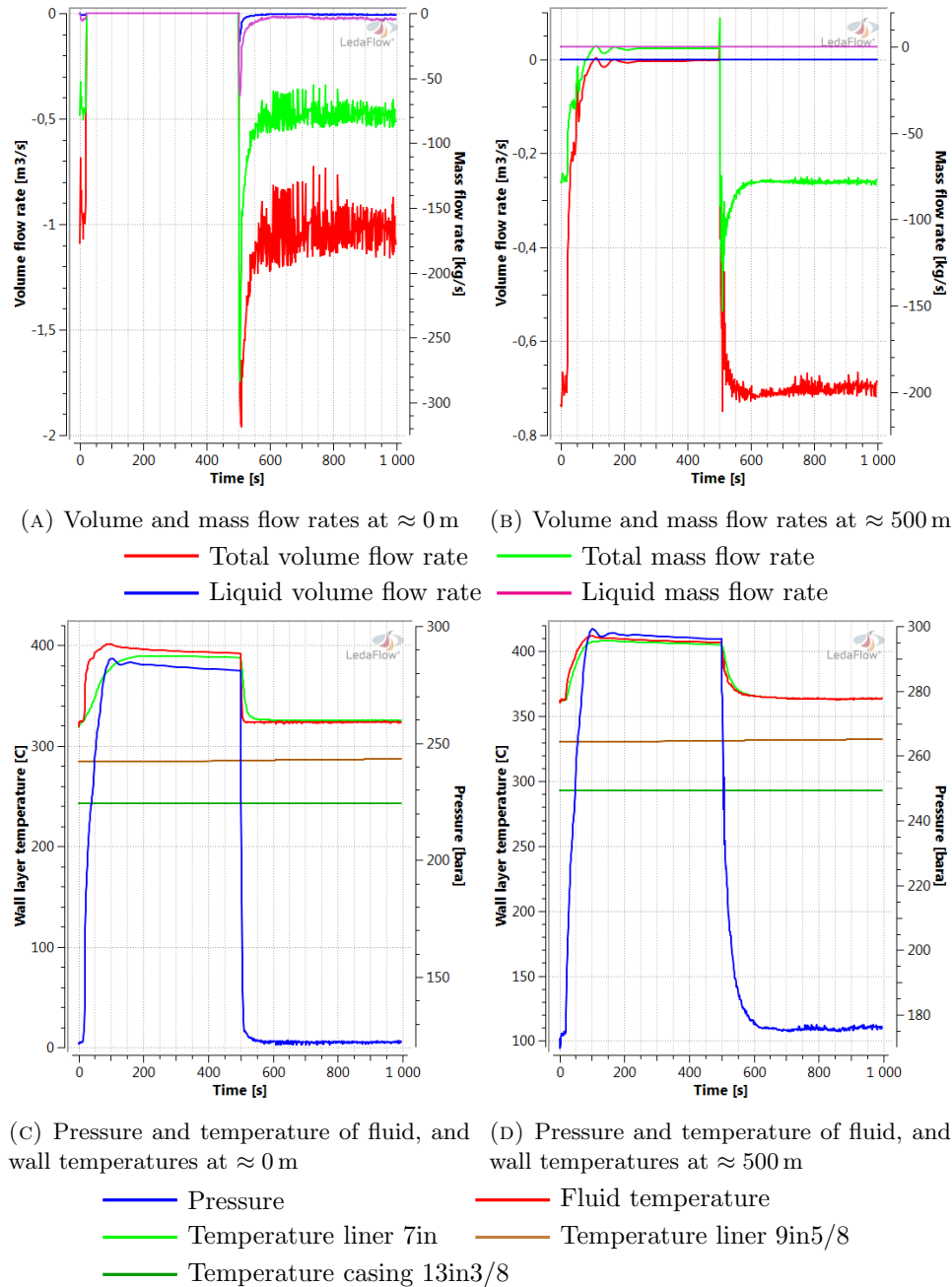- Temperature casing 13in3/8

FIGURE 4.7. Well behaviour during restart from warm well

this will be overcome and commercial production will be in focus, tools to design and operate the wells will be required. In particular, though production will most probably be in single phase, two-phase water-steam transients cannot be excluded during start-up or shut-in phases, as well as unplanned events.

The pipe multiphase flow simulator LedaFlow, developed initially for the the Oil and Gas industry, is very well suited to perform these tasks. In the present article, we have demonstrated that we are able to simulate relevant steady-state and transient events in the well, including the dynamic coupling with the surrounding

rock temperature. Some instabilities related to the supercritical water properties remain, thus further work is required to improve robustness for simulation of water systems through the critical point.

In steady-state production, we are able to estimate the flow rate in the well, as well as the temperature at well head, which can be used for sensitivity studies and to dimension the well. The pressure-temperature profile of the water in the well can be retrieved, to predict whether a given set of conditions will lead to dry or wet steam production.

With some examples of start-up and shut-in cases, we can show that it may not be possible to avoid operating the well through regions of multiphase flow. Predicting when this happens may be crucial not to damage equipment not designed to withstand droplets in steam. In addition, the large temperature variations have a strong effect on water or steam density in supercritical region, which can have an effect on the pressure response of the well.

Acknowledgment

References

[1] GEOELEC project, *Towards more geothermal electricity generation in Europe*, 2014. Accessible at `http://www.geoelec.eu/wp-content/uploads/2014/01/GEOELEC-report-web.pdf`

[2] Descramble project, under the European H2020 framework, website: `http://www.descramble-h2020.eu`

[3] International Energy Agency, *Technology Roadmap – Geothermal Heat and Power*, 2011. Accessible at `https://www.iea.org/roadmaps/`

[4] Alexandre Goldszal, Jon Ingar Monsen, Thomas J. Danielson, Kris M. Bansal, Z. L. Yang, Stein. T. Johansen and Guy Depay, *LedaFlow 1D: Simulation results with multiphase gas/condensate and oil/gas field data*, proceedings of the 13$^{\text{th}}$ International Conference on Multiphase Production Technology, Edinburgh, UK, 13–15 June 2007.

[5] Harald Laux, Ernst Meese, Sjur Mo, Tor Erling Unander, Stein Tore Johansen, Kris M. Bansal, Thomas J. Danielson, Alexandre Goldszal and Jon Ingar Monsen, *Multidimensional Simulations of Multiphase Flow for Improved Design and Management of Production and Processing Operation*, proceedings of the 2008 Offshore Technology Conference, Houston, Texas, U.S.A., 5–8 May 2008.

[6] Jørn Kjølaas, Andrea Shmueli, Alexandre Morin, *Liquid loading and multiple solutions in vertical flows – experiments and modelling with LedaFlow*, proceedings of the 10$^{\text{th}}$ North American Conference on multiphase technology, Banff, Canada, 8–10 June 2016.
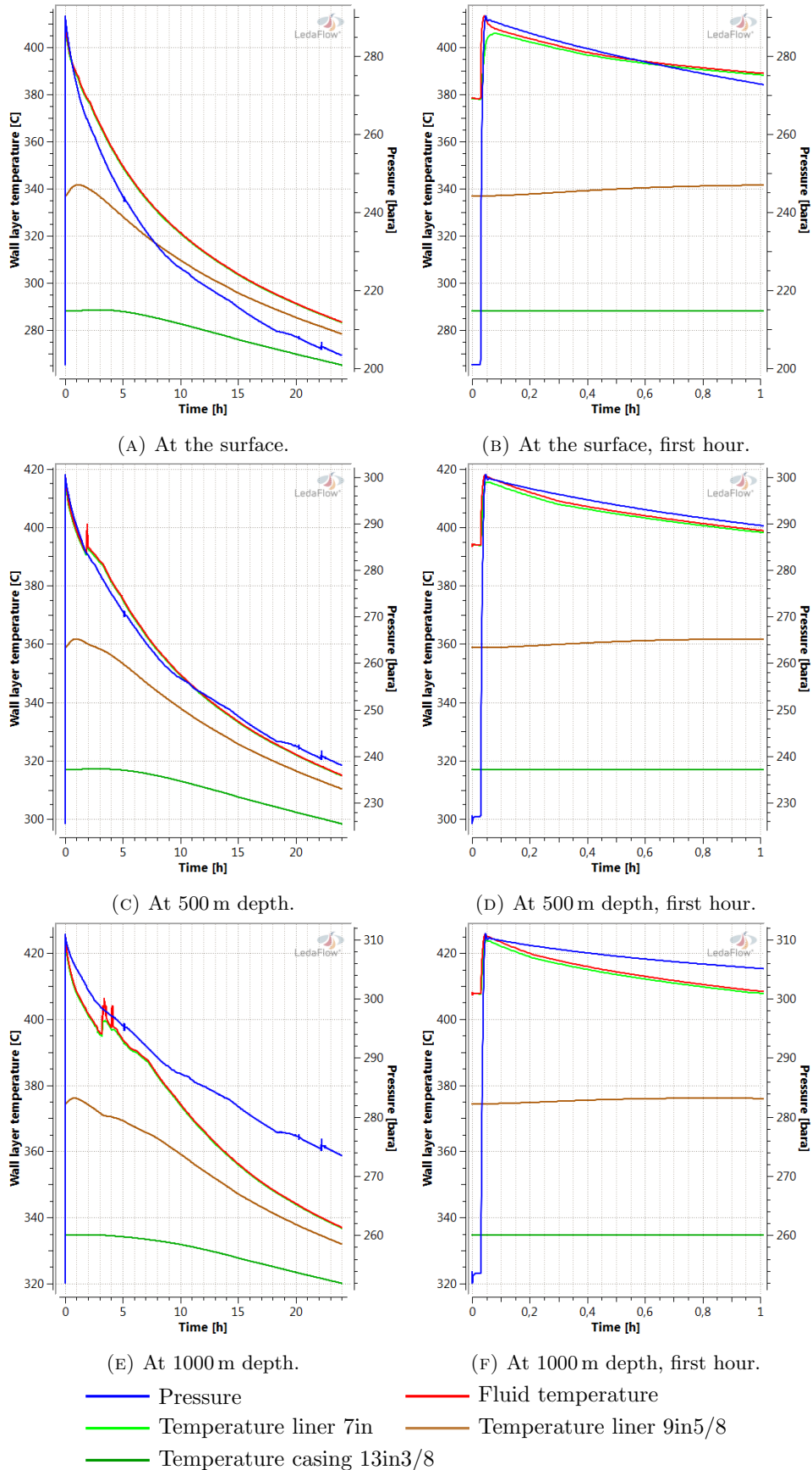
(A) At the surface.

(B) At the surface, first hour.

(C) At 500 m depth.

(D) At 500 m depth, first hour.

(E) At 1000 m depth.

(F) At 1000 m depth, first hour.

— Pressure   — Fluid temperature

— Temperature liner 7in   — Temperature liner 9in5/8

— Temperature casing 13in3/8

FIGURE 4.8. Pressure and temperature evolution during shut-in at 350 bar bottomhole pressure and 200 bar wellhead pressure.

(A) At the surface.

(B) At the surface, first hour.

(C) At 500 m depth.

(D) At 500 m depth, first hour.

(E) At 1000 m depth.

(F) At 1000 m depth, first hour.

Pressure — Fluid temperature

Temperature liner 7in — Temperature liner 9in5/8
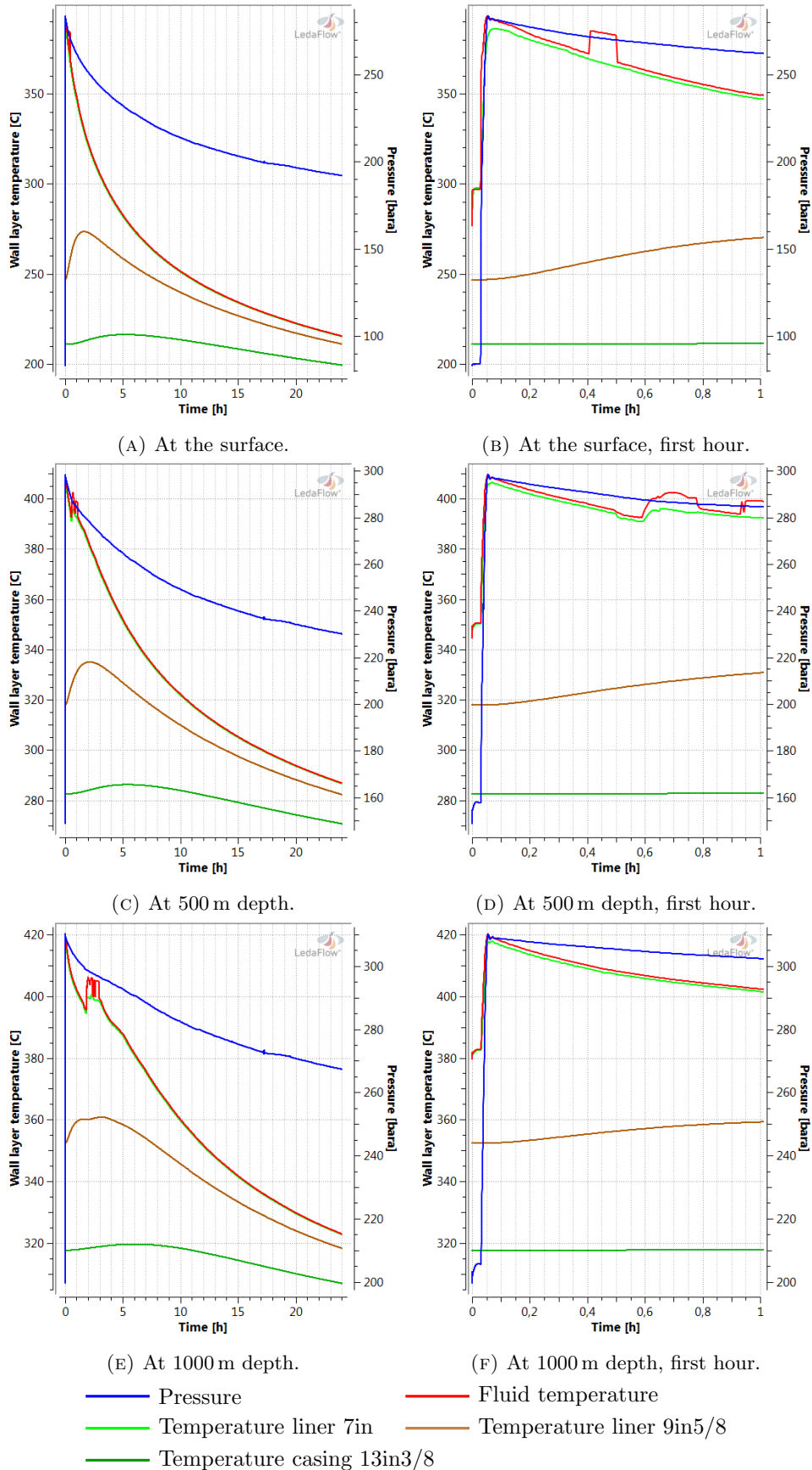
Temperature casing 13in3/8

FIGURE 4.9. Pressure and temperature evolution during shut-in at 350 bar bottomhole pressure and 80 bar wellhead pressure.